Talanta 91 (2012) 26–32

Contents lists available at SciVerse ScienceDirect

Talanta

journal homepage: www.elsevier.com/locate/talanta

New tetradecyltrimethylammonium-selective electrodes: Surface composition and topography as correlated with electrode's life span

Hayat M. Marafie*, Tahani F. Al-Shammari, Adel F. Shoukry

Chemistry Department, Faculty of Science, Kuwait University, P.O. Box 5969 Safat, 13060 Kuwait, Kuwait

ARTICLE INFO

Article history:
Received 3 October 2011
Received in revised form 5 December 2011
Accepted 6 December 2011
Available online 19 December 2011

Keywords:
Tetradecyltrimethylammonium
Polyelectrolyte
Ion-selective electrode
X-ray photoelectron spectroscopy
Electron microscopy

ABSTRACT

Two conventional plastic membrane electrodes that are selective for the tetradecyltrimethylammonium cation (TTA) have been prepared. The ion exchangers of these sensors were the ion associate, TTA-PT, and the ion aggregate, TTA-PSS, where PT and PSS are phosphotungstate and polystyrene sulfonate, respectively. The following performance characteristics of the TTA-PT- and TTA-PSS-containing electrodes were found: conditioning time of 30 and 20 min; potential response of 58.2 and 61.1 mV/TTA concentration decade; rectilinear concentration ranges of 2.0×10^{-5}–5.0×10^{-2} and 1.5×10^{-5}–7.9×10^{-2} mol L^{-1}; average working pH ranges of 4.0–10.5 and 3.8–10.7; life spans of 20 and 28 weeks, and isothermal temperature coefficients of 4.44×10^{-4} and 6.10×10^{-4} V/°C, respectively. Both electrodes exhibited high selectivity for TTA with an increasing number of inorganic and quaternary ammonium surfactant cations. These electrodes have been successfully applied to assay an antiseptic formulation containing TTA. Surface analyses using electron microscopy and X-ray photoelectron spectroscopy were used to determine the cause of the limited life span of plastic membrane electrodes.

1. Introduction

Cationic surfactants are widely used in the manufacture of many commercial products and pharmaceutical formulations, including textile softeners, anti-corrosion agents, disinfectants, cosmetics and household cleaning products [1–4]. However, the growing consumption of these compounds has a negative environmental impact. This resulted in growing concern to establish procedures to detect and monitor these compounds in the environment and to assay them in products for quality control purposes. Tetradecyltrimethylammonium bromide (TTAB) is one of the most important cationic surfactants. It has diverse applications especially as a preservative in many cosmetic and pharmaceutical products and as an effective antiseptic compound [5]. Many patents [6] have been reported that describe the cleaning formulations composed of TTAB, a chelant, and alcohol solvent mixtures. TTAB has also been a main component in lysing reagent for blood analysis [7]. Therefore, a simple and reliable technique is needed to determine the concentration of TTAB in products for the purpose of quality control in manufacturing companies [8]. The most suitable technique for this purpose is potentiometric sensing. Although many ion-selective electrodes have been developed for surfactants in the last three decades [9–12], very little has yet been reported about TTAB electrodes. A coated-wire TTAB electrode based on carboxylated PVC was constructed [13] and its response was examined over several months. However, no other performance characteristics of the electrode, such as the effect of pH, selectivity, or possible applications, were studied in this work. The purity of cetrimide, a composite containing TTAB, was analyzed [14] by an assay method according to a procedure in the European Pharmacopoeia. This method involved the conversion of TTAB to the iodide analogue (TTAI) by adding an excess of KI standard solution and back titrating with iodate solution. The TTAB concentration was also determined by titrating against a standard solution of perchloric acid [15] and silver nitrate [16]. It is evident that these methods do not allow for the direct determination of the presence of TTAB and are applicable to neither in-field nor in-line analyses.

Oppositely charged surfactants and polyelectrolytes have a strong tendency to bind to one another [17]. This tendency is quantified by the critical aggregation concentration (CAC) which is the surfactant concentration at which this surfactant and the poly-charged ion begin to aggregate [18,19]. Upon mixing these two oppositely charged species, the surface tension of the surfactant/polyionic molecules mixture decreases with increasing surfactant concentration and reaches a clear break point at which the aggregate starts to precipitate. At this point the surfactant/polyelectrolyte attraction overcomes their solubility and the aggregate solid phase starts to separate from the solvent [20]. This establishes an equilibrium system between the liquid gel and the

---

* Corresponding author. Fax: +965 24816482.
E-mail address: hayat.marafie@ku.edu.kw (H.M. Marafie).

0039-9140/$ – see front matter © 2012 Elsevier B.V. All rights reserved.
doi:10.1016/j.talanta.2011.12.035

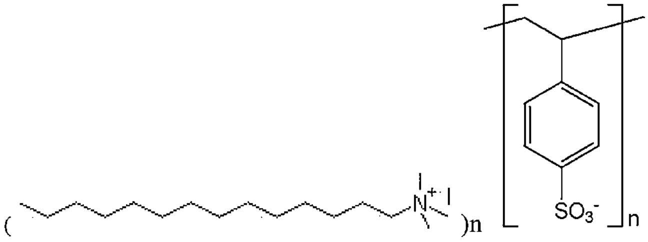

Scheme 1. TTA-PSS ion aggregate.

precipitating phase, which depends on the strength of the head groups of the poly-charged ion.

Polystyrene sulfonate (PSS) is a typical poly-charged anion of highly lipophilic polymeric chains (the degree of polymerization is 340). It interacts strongly with cationic surfactants to form aggregates at very low critical aggregation concentrations [19,21]. This is attributed to the specific hydrophobic interaction of the aromatic rings of the PSS-anion and the non-polar interior of the surfactant micelles [22].

The polyelectrolyte-surfactant aggregates have diverse applications in drug delivery, cosmetic formulations, and rheological modification [23,24]. However, none of these aggregates have yet been used as an exchanger in an ion-selective electrode, although they can provide multiple-sites for the phase boundary exchange of the targeted species. Moreover, this type of aggregate has a highly lipophilic organic part and many electrostatic bonds between TTAB and PSS.

The ion associate, hexadecypyridinium-phosphotungstate (HDP-PT) was used in 1988 as a novel exchanger in HDP-selective electrode [25]. This exchanger exhibited better performance characteristics than those electrodes based on ion pairs as the exchanger. Since 1988 many other ion associates of pharmaceutical cationic species [26–30], and surfactants [31,32], have been used for the same purpose.

The success of ion associates as exchangers was attributed to their higher lipophilicity and the greater number of sites available for ionic exchange as compared to ion pairs. In the present work, an ion aggregate composed of TTA with the polyelectrolyte, polystyrene sulfonate (PSS) is introduced as a novel exchanger for TTA in its electrode (Scheme 1). The polymeric nature of this ion aggregate makes the potential applications of this ion aggregate promising because it can provide a large number of ion exchange sites.

2. Experimental

2.1. Reagents and materials

Sodium (polystyrene sulfonate) (NaPSS) of molar mass 70,000 g/mol (Sigma Aldrich), phosphotungstic acid (PTA) (Fluka), tetradecyltrimethylammonium bromide (TTAB) (Sigma Aldrich), dioctyl phthalate (DOP) (Fluka), poly(vinyl chloride) (PVC) of high molecular weight (Fluka), tetrahydrofuran (THF) (Sigma Aldrich), and Savlon antiseptic cream (Novartis Consumer Health, Horsham, RH12 5AB, UK) were used. All aqueous solutions were prepared in bi-distilled water. The TTA-PT ion associate was prepared as previously described [25] and its purity was checked by elemental analysis. The results revealed a stoichiometric ratio of 3:1 (TTA:PT). The TTA-PSS aggregate was prepared by adding 100 mL solution containing 3.31 g (9.84 mmol) TTAB drop-wise with continuous stirring into 100 mL aqueous solution containing 2.00 g (2.85×10^{-2} mmol) of NaPSS. The spongy white precipitate was filtered and thoroughly washed with distilled water until it was free of Cl^- ions, as tested by $AgNO_3$ solution. The product was dried under vacuum and subjected to IR and elemental analyses. The results revealed the formation of ion aggregates in which more than 99% of the negatively charged sites in the PSS poly-anion are statically bonded to TTA cationic species.

2.2. Construction of the electrodes

The electrodes were prepared as previously described [26] using membranes of different compositions (Table 1).

2.3. Potentiometric measurements

The following assembly was used to measure the potential:

Ag|AgCl|internal solution|membrane|test solution||AgCl|Ag

The measuring instrument was an Orion, Model 420A pH/mV meter. A Caron circulator thermostat was used to control the temperature of the test solution. The method of obtaining the calibration graph was similar to that described previously [25].

2.4. Selectivity

The selectivity coefficients of the TTA-selective electrodes ($K_{\text{pot}}^{\text{TTA},j^{z+}}$) towards different inorganic and quaternary ammonium cationic species, j^{z+}, were determined by the separate solution (SSM) [33] and matched potential methods (MPM) [34].

2.5. Analytical application

The antiseptic cream (Savlon, Novartis Consumer Health, Horsham, RH12 5AB, UK), was assayed by applying the standard addition method using the TTA-electrodes as sensors. An accurately weighed sample of the cream was dispersed in 0.1 mol L^{-1} HNO_3 solution and the greasy material was extracted with petroleum ether. The aqueous layer containing TTA was collected using a separating funnel and its pH adjusted to 6.0 with NaOH solution; then the volume was increased to 100 mL with bi-distilled water.

2.6. X-ray photoelectron spectroscopy (XPS)

XPS spectra were recorded on a model VG ESCALAB 200 (UK) spectrometer using Mg Kα radiation (1253.6 eV) and operated at 300 W (15 kV, 20 mA). The spectra acquisition and processing were carried out by means of an Eclipse V 2.1 data system (UK). The plastic membrane of the electrode was carefully cut out and introduced into the preparation chamber with the sample holder, degassed until a pressure of about 10^{-6} Torr was achieved, and was then transferred into the analysis chamber. The analyses were carried out under the following conditions: analysis chamber pressure of 10^{-9}–10^{-10} Torr, step size of 0.1 eV, dwell time of 100 ms, pass energy of 20 eV, and a source of Mg Kα in the large-area mode. All binding energy values were determined with respect to the C 1s line (284.6 eV), which originates from adventitious carbon. The depth profiling was performed with an Ar ion gun with 5 kV energy and a 1 μA sample current.

2.7. Electron microscopy

The surface topography of membranes cut from new and exhausted electrodes was studied by a ZEISS-variable pressure field emission scanning electron microscope model SUPRA 50VP.

Table 1
Effect of membrane composition on TTA-electrode's performance.

TTA-PSS mg (%)	DOP, mg (%)	PVC, mg (%)	Slope[a]	TTA-PT mg (%)	DOP, mg (%)	PVC, mg (%)	Slope[a]
1.73 (0.25)	344.10 (49.88)	344.10 (49.88)	37.0	34.5 (5.00)	327.8 (47.50)	327.8 (47.50)	37.5
3.45 (0.50)	343.27 (49.75)	343.27 (49.75)	61.1	50.00 (7.24)	320.0 (46.38)	320.0 (46.38)	58.2
5.18 (0.75)	342.40 (49.63)	342.40 (49.63)	60.0	103.5 (15.00)	293.25 (42.50)	293.25 (42.50)	44.7
6.90 (1.00)	341.50 (49.50)	341.50 (49.50)	37.2	138.00 (20.00)	276.00 (40.00)	276.00 (40.00)	36.0

[a] mV/pTTA.

3. Results and discussion

3.1. Composition of the membranes

Membranes containing different percentages of TTA-PT ion associate or TTA-PSS ion aggregate, DOP, and PVC were measured (Table 1). When TTA-PT was used as the exchanger, the electrodes made from membranes containing 7.24% (TTA-PT) and 46.38% (w/w) of each of DOP and PVC exhibited the best response (58.2 mV/TTA concentration decade) over a concentration range of 2.0×10^{-5}–5.0×10^{-2} mol L^{-1} with a detection limit of 4.22 μg TTA/mL. For electrodes containing TTA-PSS, the optimum membrane composition was 0.5% TTA-PSS and 49.75% (w/w) of each of DOP and PVC; this electrode showed a potential response of 61.1 mV/TTA concentration decade over a concentration range of 1.5×10^{-5}–7.9×10^{-2} mol L^{-1} with detection limit of 3.23 μg TTA/mL. The latter was estimated according to IUPAC recommendation [35]. The practical response time of both electrodes was always ≤15 s. Membranes other than those with optimum compositions revealed slightly inferior analytical characteristics when used for making the sensors; thus these membranes were not considered for other studies.

3.2. Life span of the electrodes

The performance characteristics of the electrodes were investigated as a function of soaking time. For this purpose, the electrode was soaked in a 1.0×10^{-3} mol L^{-1} TTAB solution, and calibration graphs (pTTA vs. E, mV) were constructed three times every week. For electrodes based on TTA-PT, the average calibration graph slope was 58.2 mV/TTA concentration decade after 30 min of conditioning time and remained constant for 20 weeks, after which the slope started to decrease gradually. For the electrode based on TTA-PSS, the minimum conditioning time was 10 min, at which time the average calibration graph slope of 61.1 mV/TTA concentration decade was obtained. The electrode surface remained active with acceptable thermodynamic response for 28 weeks. After this interval, the electrode started to lose its activity and the calibration graph slope decreased gradually.

From the above results, it is evident that the life span of electrode employing TTA-PSS as exchanger is longer than that containing TTA-PT. This is most plausibly due to the polymeric nature of PSS, which enhances the interconnection between the ion exchanger, TTA-PSS, and the PVC polymeric network via the solvent mediator.

3.3. Effect of pH

The stability of the sensor's potential reading was investigated over a wide pH range to determine the working pH range of each of the two electrodes. The investigations were performed in TTAB solution at two concentrations: 6.0×10^{-4} and 1.0×10^{-3} mol L^{-1}. The pH values were adjusted with solutions of NaOH and HCl (0.1–1.0 mol L^{-1} each). There were no significant variations in the potential reading within the pH range of 4.0–10.5 in the case of (TTA-PT)-based electrode and within the pH range of 3.8–10.7 in the case of (TTA-PSS)-based electrode (Fig. 1). In these ranges the electrodes can be safely used for TTA determination without using buffer solutions. Both electrodes showed the same trend of potential changes before and after their pH ranges, as shown in Fig. 1. The decrease in potential in the acid medium may be attributed to the disturbance of the TTA-exchange equilibrium at the phase boundary zone, as a result of hydronium ion penetration into the gel layer of the membrane. At higher pH-ranges, the increase in potential (Fig. 1) is most plausibly due to the interference of sodium ions.

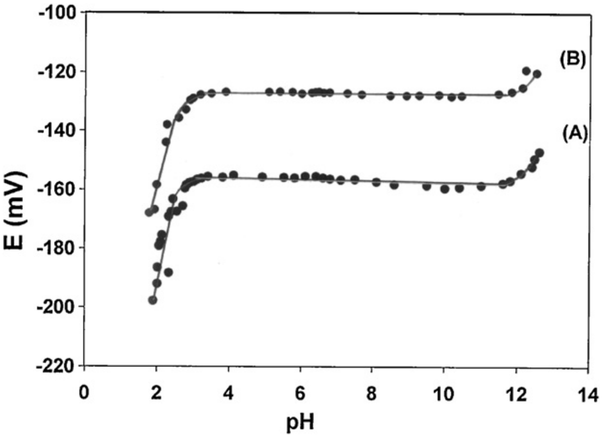

Fig. 1. Effect of pH of TTA solution on the cell potential using electrode based on TTA-PSS ion associate. (A) $C_{TTA} = 2.0 \times 10^{-4}$ mol L^{-1} and (B) $C_{TTA} = 6.0 \times 10^{-5}$ mol L^{-1}.

3.4. Selectivity

The ability of the prepared electrodes to respond to the TTA quaternary cation in the presence of other cationic species was investigated by determining the selectivity coefficient values of the electrodes; for this purpose the separate solution (SSM) [33] and matched potential methods (MPM) [34] were applied. The results (Table 2) showed that in most cases, the values obtained by the two methods were slightly different. This may be attributed to the fact that the SSM, in contrast to the MPM, is based on the Nikolsky equation [36,37], which assumes Nernstian behavior of the interfering species.

Two main categories of cations were considered, namely inorganic cations and organic ammonium cations. The selectivity coefficients obtained (Table 2) revealed that the electrodes are selective for TTA towards the investigated inorganic cations. This may be attributed to the difference in lipophilicity between TTA and these cations in addition to the difference in the magnitude of the cationic charge in the case of divalent and trivalent cations. As for the quaternary ammonium cations, DDTA, DTA, TBDA and

Table 2
Selectivity coefficients, $K_{\text{pot}}^{\text{TTA},j^{z+}}$, of TTA-selective electrodes.

Intetrferent J^{z+}	TTA-PT electrode			TTA-PSS electrode		
	$K_{\text{pot}}^{\text{TTA},j^{z+}}$ (SSM)	$K_{\text{pot}}^{\text{TTA},j^{z+}}$ (MPM)	$K_{\text{pot}}^{\text{TTA},j^{z+}}$ Mean value	$K_{\text{pot}}^{\text{TTA},j^{z+}}$ (SSM)	$K_{\text{pot}}^{\text{TTA},j^{z+}}$ (MPM)	$K_{\text{pot}}^{\text{TTA},j^{z+}}$ Mean value
Na^+	6.0×10^{-2}	6.6×10^{-3}	3.3×10^{-2}	1.6×10^{-2}	5.4×10^{-2}	3.5×10^{-2}
K^+	7.2×10^{-3}	1.6×10^{-4}	3.7×10^{-3}	8.5×10^{-2}	1.6×10^{-2}	5.1×10^{-2}
Ag^+	9.3×10^{-3}	1.1×10^{-2}	1.0×10^{-2}	6.9×10^{-2}	1.5×10^{-2}	4.2×10^{-2}
Mg^{2+}	1.6×10^{-4}	8.4×10^{-2}	4.2×10^{-2}	9.5×10^{-4}	3.0×10^{-2}	1.5×10^{-2}
Ca^{2+}	1.3×10^{-4}	1.6×10^{-2}	8.1×10^{-3}	1.3×10^{-4}	3.1×10^{-2}	1.6×10^{-2}
Ba^{2+}	7.9×10^{-4}	4.1×10^{-2}	2.1×10^{-2}	1.2×10^{-3}	5.7×10^{-2}	2.9×10^{-2}
Ni^{2+}	1.3×10^{-4}	6.5×10^{-2}	3.3×10^{-2}	8.1×10^{-4}	3.5×10^{-2}	1.8×10^{-2}
Cu^{2+}	1.0×10^{-4}	1.4×10^{-2}	7.1×10^{-3}	9.7×10^{-4}	3.6×10^{-2}	1.8×10^{-2}
Co^{2+}	1.6×10^{-4}	1.6×10^{-2}	8.1×10^{-3}	1.2×10^{-3}	4.8×10^{-2}	2.5×10^{-2}
Cd^{2+}	1.0×10^{-4}	1.7×10^{-2}	8.6×10^{-3}	1.0×10^{-3}	4.6×10^{-2}	2.4×10^{-2}
Zn^{2+}	2.0×10^{-4}	1.0×10^{-2}	5.1×10^{-3}	1.1×10^{-3}	4.1×10^{-2}	2.1×10^{-2}
Pb^{2+}	2.0×10^{-4}	–	2.0×10^{-4}	1.2×10^{-3}	3.2×10^{-2}	1.7×10^{-2}
Hg^{2+}	1.3×10^{-4}	9.5×10^{-2}	4.8×10^{-2}	6.6×10^{-4}	–	6.6×10^{-4}
Fe^{3+}	2.5×10^{-4}	4.8×10^{-2}	2.4×10^{-2}	2.8×10^{-4}	1.2×10^{-2}	6.1×10^{-3}
DDTA[a]	9.5×10^{-2}	1.0×10^{-2}	5.3×10^{-2}	1.2×10^{-2}	1.0×10^{-2}	1.1×10^{-2}
DTA[b]	7.2×10^{-3}	1.4×10^{-2}	1.1×10^{-2}	4.0×10^{-3}	3.7×10^{-2}	2.1×10^{-2}
TBDA[c]	1.2	9.7×10^{-1}	1.1	2.1	1.6	1.9
HBDA[d]	1.9×10^{-1}	6.8×10^{-3}	9.8×10^{-2}	8.9×10^{-1}	8.0×10^{-3}	4.5×10^{-1}

[a] Dodecytrimethyl ammonium.
[b] Decyltrimethyl ammonium.
[c] Tetradecybenzyldimethyl ammonium.
[d] Hexadecylbenzyldimethyl ammonium.

HBDA (Table 2), the electrodes showed mean selectivity coefficient values of 5.3×10^{-2}, 1.1×10^{-2}, 1.1, and 9.8×10^{-2}, respectively, for the TTA-PT based electrode; and 1.1×10^{-2}, 2.1×10^{-2}, 1.9 and 4.5×10^{-1}, respectively, for the TTA-PSS based electrode. These data show that the selectivity coefficients for the TTA-PT- and TTA-PSS-based electrodes follow the order: TBDA > HBDA > DDTA > DTA and TBDA > HBDA > DDTA ≈ DTA, respectively. The poor selectivity in the case of TBDA is most plausibly due to the presence of the tetradecyl radical as main branch in the structures of both TTA and TBDA, which results in a similarity in the steric character of the two species. This led to a similarity in the distribution of the effective charge on the surfaces of the two cations. In the case of HBDA, the main branch of the quaternary ammonium cation is the hexadecyl radical which is close but not identical, in structure to the tetradecyl radical of TTA. This result explains the smaller selectivity coefficients obtained for HBDA than those obtained in the case of TBDA.

3.5. *Analytical application*

The standard addition method was applied to test for TTAB in pure solution and in the antiseptic cream, Savlon, using the electrodes as sensors (Table 3). In this method. small aliquots of a 0.1 mol L^{-1} standard solution of TTAB were added to pure TTAB solution or to a solution of cream extract. The sample content of TTA was calculated from the difference in the potential readings before and after the standard addition.

The *F*-significance test [38] was applied to compare the precision of the proposed method using pure solution with that of the cream extract. This test evaluates the random error in the presence of the matrix of the extract in comparison with that in pure solution. The ratios of variance (*F* values), s_1^2/s_2^2 (where $s_1 > s_2$), obtained for the two electrodes were less than the theoretical value at a 95% probability level [38] (Table 3). This revealed that the random error associated with the cream extract is not significantly higher than that in pure water.

3.6. *Electron microscopy*

The electron microscopy images of surfaces of fresh and expired electrodes, as obtained by tracing the secondary electrons emitted from the membrane surface, (Fig. 2) shows clear changes in the morphology of the surfaces. These changes are most plausibly due to some sort of test solution/gel phase interaction in the immediate vicinity of the boundary junction that separates the membrane surface from the bath solution. This interaction is certainly associated with the leaching process of the active ingredient from the membrane's surface. In the TTA-PT electrode case, the soft surface of the fresh membrane (Fig. 2A) suffered from surface cracking as a result of the prolonged soaking (Fig. 2B), while for the TTA-PSS electrode, the smooth surface of the fresh membrane (Fig. 2C) turned coarse with some symmetrical net-work (Fig. 2D). The difference in the surface morphology of the two expired electrodes (Fig. 2 B and D) is definitively attributed to the difference in the nature of the counter anionic species of the ion exchangers. The gel layer of the TTA-PSS electrode has a much lower surface tension than the corresponding layer of the TTA-PT electrode. This is due to the existence of the aggregate, which leads to more diffusion of water molecules into the swelled polymeric network than in the TTA-PT electrode.

It is evident that the limitation of life span of the electrodes is attributed to the active ingredient leaching out, as will be observed from the XPS studies, in addition to the morphological change of the surface. The harm of these surface changes is that they generate unequal strains at the deformed areas, which consequently produces asymmetry potentials [39]. These potentials contribute to the total potential of the surface at the phase-separating boundary and negatively affect the performance of the sensor.

3.7. *X-ray photoelectron spectroscopy*

In this technique, the spectrum is a combination of an overall trend due to resonance structures that derive from core electronic states of the elements under analysis, transmission characteristics of the spectrometer, and the energy loss process within the sample. The resonance (intrinsic) peaks together with the background features of the spectrum offer information about the chemical composition of the sample (electrode's membrane) surface.

3.7.1. *Spectra of membrane containing TTA-PT*

Fig. 3 exhibits the XP spectral bands of W(VI) (Fig. 3A) and N (Fig. 3B) for fresh and expired membranes containing the TTA-PT ion associate. Tungsten and nitrogen were focused elements

Table 3
Applying the TTA-responsive electrode to determination of TTA in its pure solution and in the antiseptic cream, Savlon, using the standard addition method.

Ion exchanger	Sample	mg taken	mg found (mean)[a]	$s^{b} \times 10^{2}$	s_{R}^{c} (%)	Recovery (%)	F^{d} value
TTA-PT	Pure solution	1.682	1.685	3.8	2.26	100.2	5.00
TTA-PT	Cream	0.841	0.810	1.7	2.15	96.3	
TTA-PSS	Pure solution	1.682	1.660	3.2	1.93	98.7	1.94
TTA-PSS	Cream	0.841	0.800	2.3	2.93	95.1	

[a] Four measurements.
[b] Standard deviation (four measurements).
[c] Coefficient of variation.
[d] $F_{\text{theoretical}} = 9.28$ (degrees of freedom $\upsilon_1 = 3$ and $\upsilon_2 = 3$).

because these can act as tracer elements for PT and TTA, respectively, in the ion associate. From the spectra in Fig. 3A, it is evident that the counts due to W(VI) 4 f5 and W(VI) 4 f7 for the fresh membrane are much higher than those in the expired membrane. The quantification of these spectra showed that the atomic percent of tungsten decreased from 9.39% for fresh membrane to 3.2% for the expired membrane. This indicates that the limitation of the life span of the electrode is attributed to the ion associate leaching into the bath solution.

Fig. 3B reveals that the counts due to N 1s core electrons increased slightly as a result of soaking, and did not decrease as they did for W. The quantification of the spectra showed that the atomic percent of N increased from 2.07% for the fresh surface to 2.93% for the expired membrane. This increase may be explained on the basis that the rate of adsorption of the TTAB surfactant molecules during soaking exceeds that of the leaching process. This has been confirmed by the appearance of a Br 3d band at a binding energy of 67.48 eV in the survey spectrum of the expired membrane.

Fig. 3A and B also indicate that all spectral bands suffered a shift to higher binding energies values as a result of soaking. This may be attributed to the change in the electrostatic environment of the elements under consideration, which occurs when gel layers form on the surfaces of used electrodes as a result of the hydration process.

3.7.2. *Spectra of membrane containing TTA-PSS*

The core electron XP spectral bands of sulfur and nitrogen have also been studied (Fig. 4) because these two elements may act as tracers for PSS and TTA, respectively. As shown in Fig. 4, it is evident

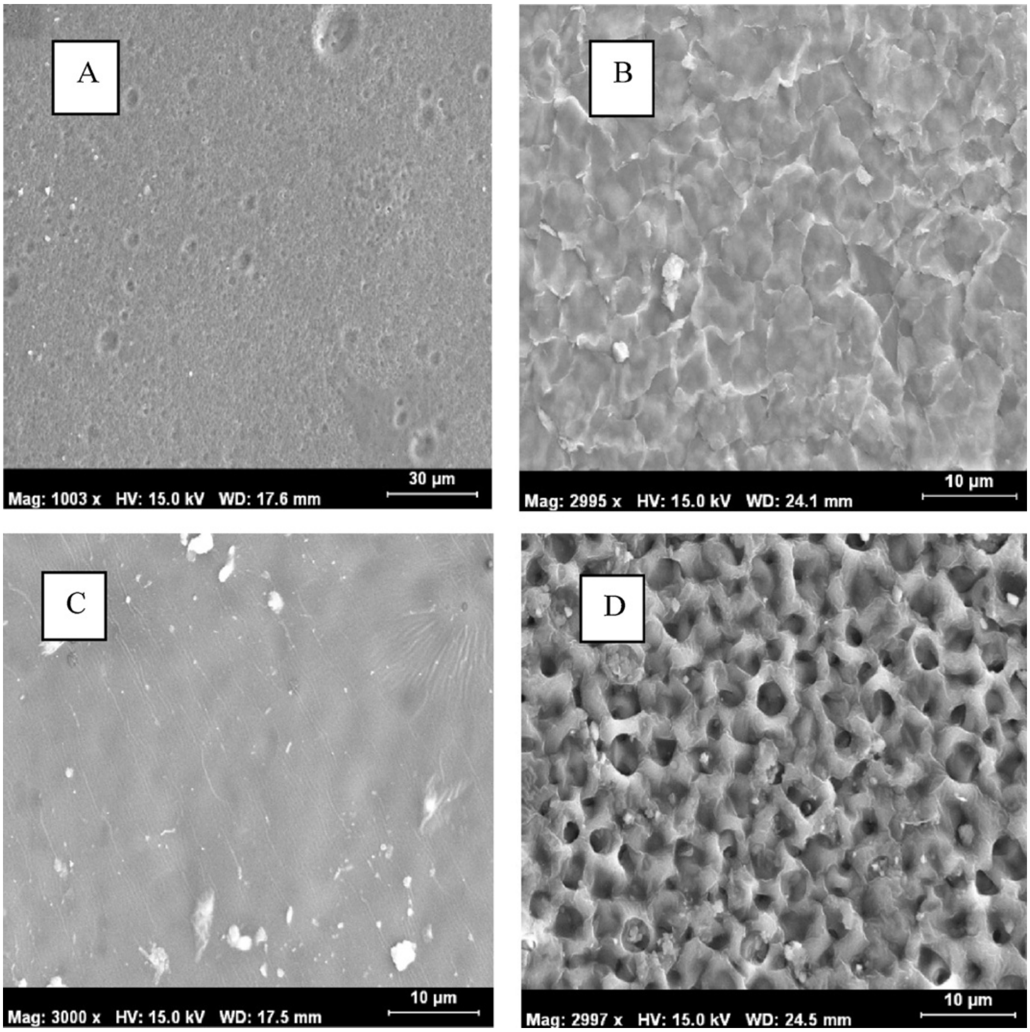

Fig. 2. High-resolution electron micrographs of membranes' surfaces and (B): fresh and expired (TTA-PT)–containing membranes, respectively. and (D): fresh and expired (TTA-PSS)–containing membranes, respectively.

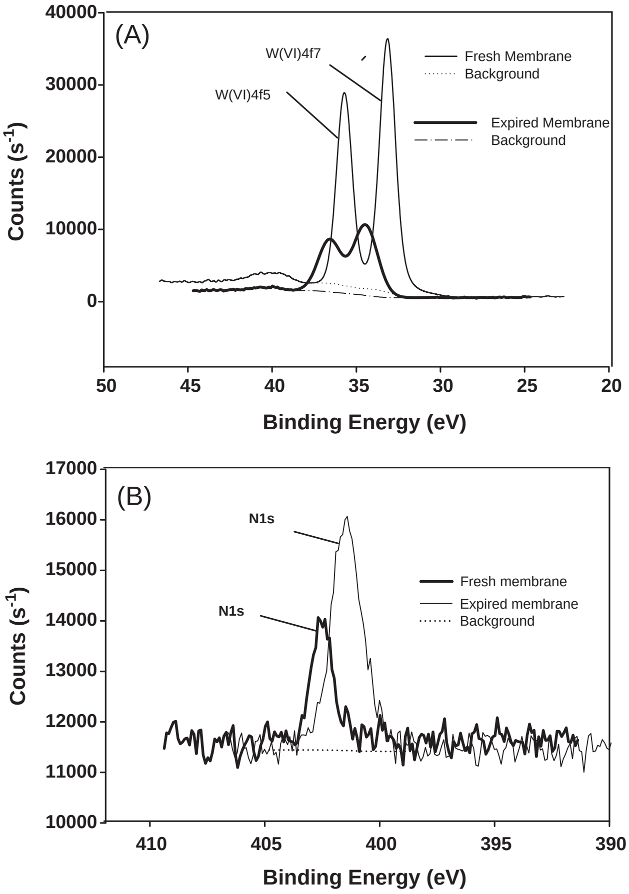

Fig. 3. X-ray photoelectron spectra characterizing W(VI)4f, A, and N 1s, B, core electrons in membranes of TTA electrode containing TTA-PT ion associate.

that the S 2p band of the expired membrane has a much smaller magnitude than that of the fresh membrane (in Fig. 4A, the atomic % of S decreased from 0.48% to 0.30%). This indicates that the limitation of the life span of the electrode is attributed to the ion aggregate TTA-PSS leaching from the external gel layer of the membrane into the test solution. On the other hand, the counts due to N 1s core electrons, increased because of soaking (in Fig. 4B, the atomic % of N raised from 0.55% to 1.95%). This may be attributed to adsorption of the TTAB surfactant molecule to the gel surface of the membrane at a rate that exceeds the loss of TTA-PSS into the bath solution. As in the case of (TTA-PT)-based electrode, the electrostatic environment affecting the concerned elements in the expired membrane is different from that in the fresh surface, which resulted in the bands shifting to higher binding energies (Fig. 4). This may be attributed to adsorption of TTAB at the hydrated surface of the expired electrode.

It is also noticeable from Fig. 4 that the N 1s and S 2p core electrons spectra of the expired membranes suffer high backgrounds that are associated with Plasmon structures. This is due to the coarse configuration of the surface (Fig. 2D), which allows for the penetration of the X-rays into greater depths. Thus, electrons emitted from the in-depth layers undergo inelastic collisions, which lead to more background counts that are associated with the appearance of extrinsic peaks (Plasmon structure).

3.8. *Effect of temperature*

The effect of temperature on the potential of ion-selective electrode is a rather complicated relationship that cannot be simply quantified as dE/dT because the temperature effect is different at

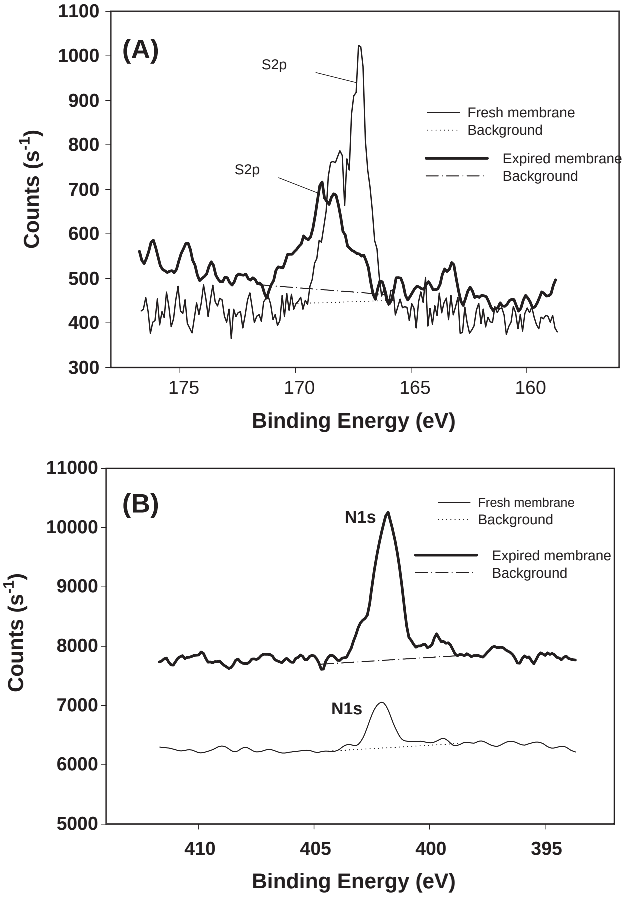

Fig. 4. X-ray photoelectron spectra characterizing S 2p, A, and N 1s, B, core electrons in fresh and expired membranes containing TTA-PSS ion aggregate.

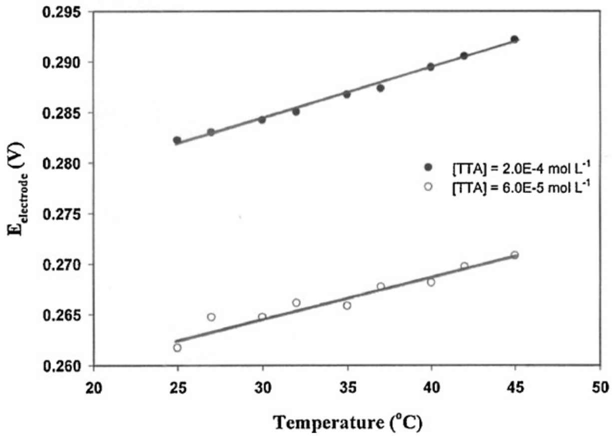

Fig. 5. Effect of temperature on potential of TTA-selective electrode based on TTA-PT ion associate.

various concentrations and is also affected by the change in reference electrode potential. Moreover, the electrode response, the liquid junction potential, and the solubility of salts in the system all vary with temperature. However, the effect of temperature change on the electrode potential can be fairly quantified in terms of dE^{o}/dT, the isothermal temperature coefficient. Fig. 5 shows the variation of the TTA-electrode's potential as a function of test solution temperature (6.0×10^{-5} and 2.0×10^{-4} mol L^{-1}). The electrode potential was calculated from the cell potential and the potential of the reference Ag/AgCl electrode at the given temperature. The latter was calculated [40] using the following equation:

$$E_{\mathrm{Ag/AgCl}} = 0.23695 - 4.8564 \times 10^{-4}\,T - 3.4205 \times 10^{-6}\,T^2 - 5.869 \times 10^{-9}\,T^3$$

where T is the test solution temperature in °C. The isothermal temperature coefficient dE^{o}/dT of the electrode was determined using the equation:

$$\frac{dE^{o}}{dT} = \frac{dE}{dT} - \left(\frac{2.303R}{F}\right)\log[\mathrm{TTA}]$$

where dE/dT is the slope of the electrode potential/temperature straight-line relationship (Fig. 5). The activity of the species has been replaced by concentration term because the medium is highly diluted.

The average isothermal temperature coefficients of the electrodes, as calculated from the straight lines obtained (Fig. 5) and the above equation were 4.44×10^{-4} and 6.10×10^{-4} V/°C, for TTA-PT- and TTA-PSS-based electrodes, respectively.

4. Conclusion

The ion associate and ion aggregate of tetradecyltrimethylammonium (TTA) cation with phosphotungstate and the polystyrene sulfonate polyanion were used successfully as cation exchangers for TTA-selective plastic membrane electrodes. The electrode based on the ion aggregate exhibited a longer life span than that based on the ion associate. This is probably due to an interaction between the two polymeric networks of PSS and PVC that is mediated by the solvent. Surface analysis results showed that the limitation of the life span of plastic membrane electrodes for cationic surfactants is due to topographical change at the electrode surface in addition to leaching of the active ingredient from the membrane's surface to the bath solution.

Acknowledgements

The supports of the University of Kuwait received through the College of Graduate Studies, the facilities of ANALAB (grant no. GS01/01), SAF (grant no. GS03/01), and the X-ray Photoelectron Spectroscopy unit and the Nanoscopy Science Center are gratefully acknowledged.

References

[1] D. Madunic-Cacic, M. Sak-Bosnar, O. Galovic, N. Sakac, R. Matesic-Puac, Talanta 76 (2008) 259–264.
[2] S.R. Patil, A.K. Rakshit, Anal. Chim. Acta 518 (2004) 87–91.
[3] J. Texter, T.A. Hatton, Curr. Opin. Colloid Interface Sci. 7 (2003) 253–254.
[4] Z. Abdel Hamid, T.Y. Soror, H.A. El-Dahan, A.M.A. Omar, Anti-Corros. Method M 45 (1998) 306–311.
[5] O. Bronocova, Folia Microbiol. 9 (1964) 201.
[6] E. Jenevein, S. Vercellotti, J. Vercellotti, C.A. 141 (2004) 192285, U.S. Pat. Appl. Publ. 110 (2004) 649.
[7] K. N. Matsuda, A. E. Shinkai, U.S. Patent 4, 617 (1986) 275, October 14, 1986.
[8] C. Gabrielli, P. Hemery, P. Letellier, M. Masure, H. Perrot, M. Rahmi, M. Turmine, Electrochim. Acta 47 (2002) 2117–2126.
[9] A. Craggs, G.J. Moody, J.D.R. Thomas, J. Chem. Educ. 51 (1974) 541–544.
[10] C.R. Martin, H. Freiser, Anal. Chem. 52 (1980) 562–564.
[11] J. Sirieix-Plenet, M. Turmine, P. Letellier, Talanta 60 (2003) 1071–1078.
[12] M. Mokus, U. Kragh-Hansen, P. Latellier, M. Maire, J.V. Moller, Anal. Biochem. 264 (1998) 34–40.
[13] R. Xu, D.M. Bloor, Langmuir 16 (2000) 9555–9558.
[14] European Pharmacopoeia 4, European Directorate for the Quality of Medicines (EDQM), Brusels, procedure 0378, 1997, 2, 585.
[15] L. Levi, P.M. Oestreicher, C.G. Farmilo, United Nations Bulletin 1953, 1, 45; http://www.unodc.org/unodc/bulletin/bulletin_1953-01-01_1_page004.html.
[16] C.D. Rasmussen, H.B. Nielsen, J.E.T. Andersen, PDA J. Pharm. Sci. Technol. 60 (2) (2006) 104–110.
[17] P. Hansson, Langmuir 17 (2001) 4167–4180.
[18] E.D. Goddard, Colloids Surf. 19 (1986) 301–329.
[19] P. Hansson, M. Almgren, Langmuir 10 (1994) 2115–2124.
[20] Y.L. Wang, K. Kimura, P.L. Dubin, W. Jaeger, Macromolecules 33 (2000) 3324–3331.
[21] K. Hayakwak, J.C.T. Kwak, in: D. Rubingh, P.M. Holland (Eds.), Cationic Surfactants: Physical Chemistry. Surfactant Science Series, Marcel Dekker Inc., New York, 1991.
[22] Z. Gao, J.C.T. Kwak, R.E. Wasylishen, J. Colloid Interface Sci. 126 (1988) 371–376.
[23] D.M. Kuntz, Dilute and Concentrated Phase Behavior of Water-soluble Rodlike Polyelectrolyte Surfactant Aggregate, ProQuest LLC, USA, 2008, pp. 1.
[24] Y. Lapistsky, E.W. Kaler, Colloid Surf. 250 (2004) 179–187.
[25] A.F. Shoukry, S.S. Badawy, R.A. Farghali, Anal. Chem. 60 (21) (1988) 2399–2402.
[26] A.F. Shoukry, M.S. Rizk, H.M. Abdel-Fattah, Y.M. Issa, E.M. Atia, J. Chem. Technol. Biotechnol. 60 (2) (1994) 217–222.
[27] Y.M. Issa, N.T. Abdel-Ghani, A.F. Shoukry, H.M. Ahmad, Mikrochim. Acta 132 (1999) 83–88.
[28] A.F. Shoukry, H.M. Marafie, L.A. Alshatti, Electroanalysis 18 (2006) 779–785.
[29] A.L. El-Ansary, Y.M. Issa, A.S. Tag-Eldin, Electroanalysis 13 (14) (2001) 1203–1208.
[30] G.A. Mostafa, S.S. Ghazy, Ann. Chim. 93 (2003) 691–699.
[31] S.S. Badawy, A.F. Shoukry, R.A. Farghaly, Microchem. J. 40 (1989) 181–186.
[32] G.G. Mohamed, T.A. Ali, M.F. El-Shahat, A.M. Al-Sabagh, M.A. Migahed, E. Khaled, Anal. Chim. Acta 673 (2010) 79–87.
[33] S.S. Badawy, A.F. Shoukry, Y.M. Issa, Analyst 111 (1986) 1363–1365.
[34] Y. Umezawa, K. Umezawa, H. Sato, Pure Appl. Chem. 67 (1995) 507–518.
[35] G.G. Guilbault, R.A. Durst, M.S. Frant, H. Freiser, E.H. Hansen, T.S. Light, E. Pungor, G. Rechnitz, N.M. Rice, J.J. Rohm, W. Simon, J.D.R. Thomas, Pure Appl. Chem. 48 (1976) 127–132.
[36] B.P. Nikolsky, Zh. Fiz Khim. 10 (1937) 495–503.
[37] B.P. Nikolsky, T.A. Tolmacheva, J. Phys. Chem. (USSR) 10 (1937) 504–512.
[38] G.D. Christian, Analytical Chemistry, sixth ed., John Wiley & Sons, New York, 2004, pp. 92–93.
[39] D.G. Peters, J.M. Hayes, G.M. Hieftje, Chemical Separations and Measurements, Theory and Practice of Analytical Chemistry, Saunders Co., WA, USA, 1974, pp. 364–367.
[40] A.J. Bard, R. Parson, J. Jordan, Standard Potentials in Aqueous Solution, Marcel Dekker Inc., New York, 1985.